

Fe, 10.15. Found: C, 47.81; H, 3.13; N, 12.51; Fe, 9.93. Calcd for Fe(salen)(pico),  $C_{22}H_{18}N_3FeO_4$ : C, 59.47; H, 4.09; N, 9.46; Fe, 12.57. Found: C, 58.16; H, 4.13; N, 9.47; Fe, 12.08.

The reactions of trichloroacetic acid and picric acid with  $[Fe(TPP)]_2O$  followed similar procedures.  $[Fe(TPP)]_2O$  was dissolved in chloroform and the solution brought to reflux. A large excess of trichloroacetic acid in water or picric acid in 95% ethanol was added to the solution with stirring. The solution was stirred at reflux for 15–30 min and then evaporated to about half of the original volume. Several 15-mL aliquots of  $H_2O$  were used to wash the chloroform solution. The solution was then evaporated to give the desired compound. Anal. Calcd for Fe(TPP)(tca),  $C_{46}H_{28}N_4FeO_2Cl_3$ : C, 66.48; H, 3.40; N, 6.74; Fe, 6.72. Found: C, 64.79; H, 3.46; N, 6.44; Fe, 6.45. Calcd for Fe(TPP)(pic),  $C_{50}H_{28}N_7FeO_7$ : C, 67.12; H, 3.16; N, 10.96; Fe, 6.24. Found: C, 65.74; H, 3.64; N, 10.59; Fe, 5.99.

**Physical Measurements.** Infrared spectra were recorded on a Perkin-Elmer Model 467 spectrophotometer. Samples were prepared as 13-mm KBr pellets. Low-temperature IR spectra were obtained using a Cryogenics Technology, Inc., "Spectrim" closed-cycle helium gas refrigerator with the cryocooling head equipped with KBr windows ( $50 \times 4$  mm).

Variable-temperature (4.2–269 K) magnetic susceptibility data were obtained with a PAR Model 150A vibrating-sample magnetometer. The temperature was monitored with a GaAs temperature-sensitive diode in conjunction with a  $CuSO_4 \cdot 5H_2O$  standard.

Electron paramagnetic resonance spectra were obtained with Varian E-line spectrometers using an E101 microwave bridge with a 6-in. (10 kG) magnet for X-band measurements and an E110 microwave bridge with a 12-in. (25 kG) magnet for Q-band measurements. A Varian liquid-nitrogen X-band cavity insert was used to obtain measurements at  $90 \pm 10$  K and an Air Products Heli-tran X-band liquid-helium cooling system to obtain measurements at  $8 \pm 2$  K. Temperatures for the X-band measurements were determined by employing an Ohmite carbon resistor ( $2.7 \pm 10\%$  k $\Omega$ ,  $1/8$  W). The low-temperature Q-band measurements were estimated to be at  $\sim 100$  K and were obtained by surrounding the cavity with a glass Dewar and passing liquid-nitrogen-cooled, gaseous nitrogen through the system.

Iron-57 Mössbauer measurements at 90 K were obtained on an instrument which was referred to in an earlier paper.<sup>22</sup>

Computer fittings of the magnetic susceptibility data were performed with an adapted version of the minimization program known as STEPT.<sup>23</sup> Computer fittings of the  $^{57}Fe$  Mössbauer data were performed with a modified version of a previously described program.<sup>24</sup>

**Acknowledgment.** We thank Professor P. G. Debrunner and Mr. C. R. Hill for assistance with the  $^{57}Fe$  Mössbauer work.

We are grateful for partial funding for our work from National Institutes of Health Grant HL 13652.

**Registry No.**  $[Fe(salen)(tca)]_2$ , 47892-68-2;  $[Fe(salen)(tfa)]_2$ , 24932-25-0;  $[Fe(salen)(sal)]_2$ , 65466-06-0;  $[Fe(salen)(pic)]_2$ , 65516-32-7; Fe(salen)(pico), 65466-05-9; Fe(TPP)(tca), 65466-04-8; Fe(TPP)(pic), 65466-03-7;  $[Fe(salen)]_2O$ , 18601-34-8;  $[Fe(TPP)]_2O$ , 12582-61-5; picric acid, 88-89-1; picolinic acid, 98-98-6.

**Supplementary Material Available:** Tables II–VIII giving magnetic susceptibility data (7 pages). Ordering information is given on any current masthead page.

## References and Notes

- (1) Camille and Henry Dreyfus Fellow, 1972–1977; A. P. Sloan Foundation Fellow, 1976–1978.
- (2) H. Schugar, C. Walling, R. B. Jones, and H. B. Gray, *J. Am. Chem. Soc.*, **89**, 3712 (1967).
- (3) I. A. Cohen and W. S. Caughey, *Biochemistry*, **7**, 636 (1968).
- (4) N. Sadasivan, H. I. Eberspaecher, W. H. Fuchsman, and W. S. Caughey, *Biochemistry*, **8**, 534 (1969).
- (5) E. B. Fleischer, J. M. Palmer, T. S. Srivastava, and A. Chatterjee, *J. Am. Chem. Soc.*, **93**, 3162 (1971).
- (6) W. H. Fuchsman, H. H. Bernstein, and D. P. Tempest, *Bioinorg. Chem.*, **4**, 177 (1975).
- (7) J. A. Bertrand, J. L. Breece, A. R. Kalyanaraman, G. J. Long, and W. A. Baker, Jr., *J. Am. Chem. Soc.*, **92**, 5233 (1970).
- (8) C. S. Wu, G. R. Rossman, H. B. Gray, G. S. Hammond, and H. J. Schugar, *Inorg. Chem.*, **11**, 990 (1972).
- (9) J. A. Bertrand, J. L. Breece, and P. G. Eller, *Inorg. Chem.*, **13**, 125 (1974).
- (10) J. A. Bertrand and P. G. Eller, *Inorg. Chem.*, **13**, 927 (1974).
- (11) H. J. Schugar, G. R. Rossman, and H. B. Gray, *J. Am. Chem. Soc.*, **91**, 4564 (1969).
- (12) J. A. Thich, C. C. Ou, D. Powers, B. Vasilou, D. Mastropaolo, J. A. Potenza, and H. J. Schugar, *J. Am. Chem. Soc.*, **98**, 1425 (1976).
- (13) W. Wojciechowski, *Inorg. Chim. Acta*, **1**, 319 (1967).
- (14) K. S. Murray, *Coord. Chem. Rev.*, **12**, 1 (1974).
- (15) W. O. Gillum, R. B. Frankel, S. Foner, and R. H. Holm, *Inorg. Chem.*, **15**, 1095 (1976).
- (16) M. Gerloch and F. E. Mabbs, *J. Chem. Soc. A*, 1900 (1967).
- (17) M. D. Hobday and T. D. Smith, *Coord. Chem. Rev.*, **9**, 311 (1972–1973).
- (18) M. Gerloch, J. Lewis, F. E. Mabbs, and A. Richards, *J. Chem. Soc. A*, 112 (1968).
- (19) T. Castner, Jr., G. S. Newell, W. C. Holton, and C. P. Slichter, *J. Chem. Phys.*, **32**, 668 (1960).
- (20) G. M. Bancroft, A. G. Maddock, and R. P. Randl, *J. Chem. Soc. A*, 2939 (1968).
- (21) B. Grobelny, B. Jezowska-Trzebiatowska, B. Modras, and Z. Olejnik, *Bull. Acad. Pol. Sci., Ser. Sci. Chim.*, **21**, 381 (1973).
- (22) R. G. Wollmann and D. N. Hendrickson, *Inorg. Chem.*, **16**, 723 (1977).
- (23) J. P. Chandler, Program 66, Quantum Chemistry Program Exchange, Indiana University, Bloomington, Ind.
- (24) B. L. Chrisman and T. A. Tumolillo, *Comput. Phys. Commun.*, **2**, 322 (1971).

Contribution from the Department of Chemistry,  
University of Houston, Houston, Texas 77004

## Substituent and Solvent Effects on the Electrochemical Properties of Tetra- $\mu$ -carboxylato-dirhodium(II)

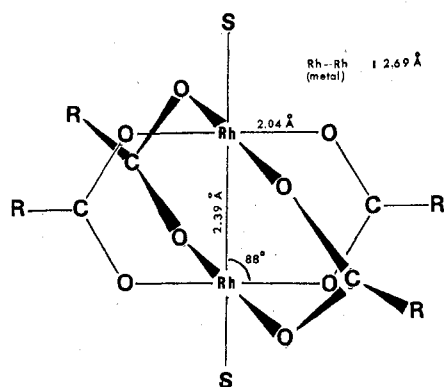
K. DAS, K. M. KADISH,\* and J. L. BEAR\*

Received July 28, 1977

The electrochemical oxidation–reduction of tetra- $\mu$ -carboxylato-dirhodium(II),  $Rh_2(O_2CR)_4$ , where  $R = (CH_3)_3C$ ,  $C_3H_9$ ,  $C_3H_7$ ,  $C_2H_5$ ,  $CH_3$ ,  $C_6H_5CH_2$ ,  $CH_3OCH_2$ ,  $C_6H_5OCH_2$ ,  $CH_3CHCl$ , and  $CF_3$  was investigated by polarography, cyclic voltammetry, and controlled potential electrolysis. At a platinum electrode  $Rh_2(O_2CR)_4$  was reversibly oxidized by a single electron to yield a stable Rh(II)–Rh(III) dimer. The same compound was irreversibly reduced in several steps but yielded initially a Rh(II)–Rh(I) dimer before further addition of one or more electrons. The half-wave potentials were found to depend on the nature of the substituent R and also the solvent. The polar substituent constants of Taft were found to bear a linear relationship with the half-wave potentials, and for a particular complex, the solvent dependency of its  $E_{1/2}$  values was shown to be roughly related to the solvent donor number.

For the past few years, we have been investigating the biological activity of several tetra- $\mu$ -carboxylato-dirhodium(II) complexes.<sup>1–3</sup> These complexes are potent inhibitors of enzymes which have sulfhydryl groups near or at the active site.<sup>4</sup>

Reaction of most sulfhydryl containing compounds with tetra- $\mu$ -carboxylato-dirhodium(II) is rapid at mid or high pH and results in a release of the carboxylate ions from the "cage" complex. The product has a complicated EPR spectra and

Figure 1. Structure of tetra- $\mu$ -carboxylato-dirhodium(II).Table I. Substituents and Values of  $4\sigma^*$ 

Compd no.	Substituent, R	$4\sigma^*^{14}$
1	$(\text{CH}_3)_3\text{C}-$	-1.20
2	$\text{c-C}_5\text{H}_9-$	-0.80
3	$n\text{-C}_5\text{H}_7-$	-0.46
4	$\text{C}_2\text{H}_5-$	-0.40
5	$\text{CH}_3-$	+0.00
6	$\text{C}_6\text{H}_5\text{CH}_2-$	+0.86
7	$\text{CH}_3\text{OCH}_2-$	+2.08
8	$\text{C}_6\text{H}_5\text{OCH}_2-$	+3.40
9	$\text{CH}_3\text{CHCl}-$	+4.20
10	$\text{CF}_3-$	$\sim 10.00$

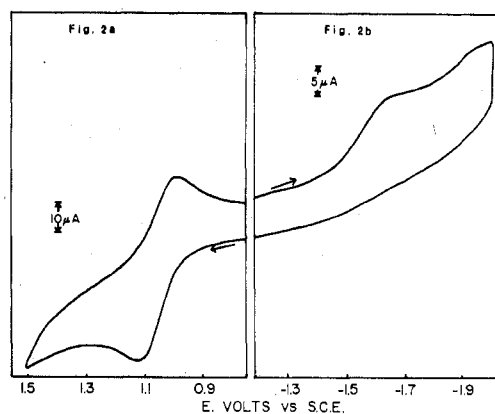
also exhibits paramagnetic line broadening in its NMR spectra.<sup>4</sup> Work is now in progress to establish the nature of this reaction. The present information indicates that electron-transfer processes are involved in the reactions. There are several reports in the literature on the redox behavior of tetra- $\mu$ -carboxylato-dirhodium(II) complexes,<sup>5-8</sup> but these involve only the acetate derivative; therefore, we have undertaken a detailed electrochemical study of different  $\text{Rh}_2(\text{O}_2\text{CR})_4$  complexes (Figure 1). In this study R was varied as shown in Table I to include a substantial range of substituent constants. Electrochemical measurements were made in both aqueous and various nonaqueous media. The purpose of this investigation was to see how substituent effects on the carboxylate ion and changes in the bonding properties of the solvent would effect the electrochemical and chemical reactivity of these complexes. This paper reports the results on the electrochemistry.

### Experimental Section

**Chemicals.**  $\text{Rh}_2(\text{O}_2\text{CCH}_3)_4$  and  $\text{RhCl}_3 \cdot 3\text{H}_2\text{O}$  were purchased from Matthey Bishop, Inc., Malvern, Pa. Other carboxylates,  $\text{Rh}_2(\text{O}_2\text{CR})_4$ , where R =  $\text{CF}_3$ ,  $\text{CH}_3\text{CHCl}$ ,  $\text{C}_6\text{H}_5\text{OCH}_2$ ,  $\text{CH}_3\text{OCH}_2$ ,  $\text{CH}_3\text{CH}_2$ ,  $\text{CH}_3\text{CH}_2\text{CH}_2$ ,  $\text{C}_6\text{H}_5\text{CH}_2$ ,  $(\text{CH}_3)_3\text{C}$ , and  $\text{C}_5\text{H}_9$ , were synthesized either from rhodium(II) acetate and the carboxylic acid or from  $\text{RhCl}_3 \cdot 3\text{H}_2\text{O}$  and an equimolar mixture of the carboxylic acid and its sodium salt in an alcoholic solution. Both the synthetic procedures and the characterization and estimation technique have been described previously.<sup>9-10</sup> The solvents methylene chloride, dimethylformamide, tetrahydrofuran, acetonitrile, benzonitrile, butyronitrile, dimethylacetamide, dimethyl sulfoxide, and pyridine were reagent grade quality. These were dried over  $\text{P}_2\text{O}_5$  and/or  $\text{CaH}_2$  and stored over molecular sieve. The solvents were made 0.1 M with tetrabutylammonium perchlorate. The supporting electrolyte for aqueous solution was 0.1 M KCl. The permissible potential range in each solvent was determined by running a blank prior to the actual run.

**Polarography and Cyclic Voltammetry.** Polarographic measurements were made on Princeton Applied Research Models 173 and 174 electrochemistry systems utilizing a three-electrode geometry. The working electrode consisted of either a dropping mercury electrode (DME) or a platinum button electrode.

A commercial calomel electrode was used as the reference electrode and a platinum wire as the auxiliary electrode. The reference electrode

Figure 2. Cyclic voltammograms of  $\text{Rh}_2(\text{O}_2\text{CC}_2\text{H}_5)_4$  in (a) DMF, 0.1 M TBAP, and (b)  $\text{Me}_2\text{SO}$ , 0.1 M TBAP. Scan rate = 0.100 V/s.

was separated from the bulk of the solution by a bridge filled with solvent and supporting electrolyte. Solutions in the bridge were changed periodically. This arrangement, thus, prevented aqueous contamination from entering the cell via the calomel electrode. The electrolysis cell was a Brinkman Model EA 875-5. Total volume utilized was 5-10 mL, and rhodium carboxylate concentrations were between  $10^{-3}$  and  $10^{-4}$  M. Linear and cyclic sweep rates were varied between 0.01 and 0.20 V/s. The overall number of electrons was determined by controlled potential coulometry. A Princeton Applied Research Model 173 potentiostat was used to control the potential at which experiments were run. Electronic integration of the current-time curve was achieved by means of a PAR Model 179 integrator, which yielded a voltage output that was recorded on an X-Y recorder. The coulometric cell was similar to that used for cyclic voltammetry. A large coiled platinum wire served as the anode and was separated from the cathodic compartment by means of a fritted disk. For reductions, a stirred mercury pool of area  $\approx 7$  cm<sup>2</sup> served as the cathode and a saturated calomel electrode was the reference electrode. Stirring of the solution was achieved by means of a magnetic stirring bar positioned atop the mercury pool and actuated by a motor beneath the cell. Deaeration of the solution was performed before commencing the experiment and a stream of high-purity argon was passed throughout. All experiments were carried out in a controlled temperature room of  $20 \pm 0.5$  °C and potentials are reported with respect to the saturated calomel electrode (SCE).

### Results

**Cyclic Voltammetry and Polarography.** The electrochemical oxidation or reduction of  $\text{Rh}_2(\text{O}_2\text{CR})_4$  proceeds in two discrete steps without destroying the dimeric cage structure of Figure 1. A typical cyclic voltammogram of  $\text{Rh}_2(\text{O}_2\text{CC}_2\text{H}_5)_4$  oxidation in DMF is shown in Figure 2a. Figure 2b shows the cyclic voltammogram for the reduction of the same compound in  $\text{Me}_2\text{SO}$ . In all cases, electrooxidation of  $\text{Rh}_2(\text{O}_2\text{CR})_4$ , where R was one of the groups in Table I, produced a single oxidation peak on the forward scan and a coupled reverse reduction peak on the backward sweep. Potential separations between the anodic peak,  $E_{p,a}$ , and the cathodic peak potential,  $E_{p,c}$ , were in the range of 60-90 mV at a scan rate of 20 mV/s and increased with sweep rate. The ratio of the cathodic to the anodic peak current,  $i_{p,c}/i_{p,a}$ , was close to unity at all scan rates indicating the absence of coupled chemical reactions.<sup>11,12</sup> In addition, plots of  $i_p/v^{1/2}$  were constant over the lower range of sweep rates of 0.02-0.100 V/s indicating diffusion control. Diagnostic plots of  $E_p - E_{p/2}$  gave a reversible separation of  $70 \pm 10$  mV, indicative of a one-electron diffusion-controlled oxidation.

The reduction of  $\text{Rh}_2(\text{O}_2\text{CR})_4$  was not reversible as shown in Figure 2b. Diagnostic measurements of peak geometry gave a separation between peak and half-peak potential,  $E_p - E_{p/2}$ , of 125 mV compared to a  $60/n$  mV theoretical diffusion-controlled shape. This larger than 60 mV separation is characteristic of an electrode reaction in which the rate of

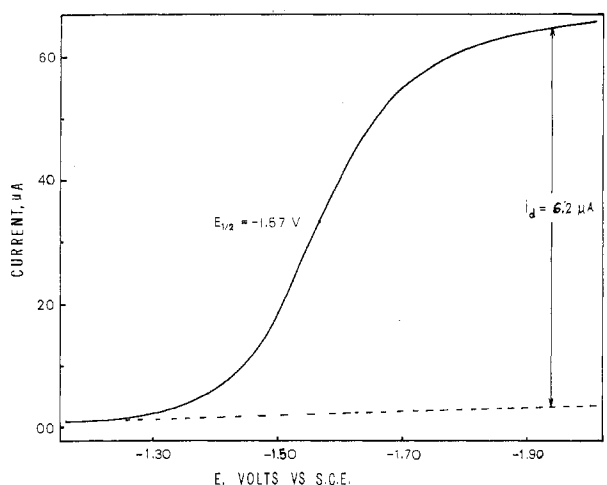


**Figure 3.** Polarogram illustrating irreversible reduction wave of  $\text{Rh}_2(\text{O}_2\text{CC}_2\text{H}_5)_4$  in  $\text{Me}_2\text{SO}$ , 0.1 M TBAP.

electron transfer is the rate-determining step.<sup>12</sup> Confirmation of this irreversibility is also seen by the lack of reverse reduction peak and the observed cathodic shift of peak potential with increase in scan rate.

For an irreversible reaction the shape of the current-voltage curve is broader than that for a reversible reaction and is given by the equation<sup>11,12</sup>

$$E_p - E_{p/2} = 0.048/\alpha n_a \text{ V} \quad (1)$$

where  $\alpha$  is the transfer coefficient and  $n_a$  is the number of electrons in the rate-determining step. Using the experimental  $E_p - E_{p/2} = 125$  mV, an  $\alpha n_a = 0.38$  was obtained from which it may be inferred that  $\alpha = 0.38$  and  $n_a = 1$ , i.e., the initial reduction step involves a rate-determining single-electron reduction.

This irreversibility and a similar value of  $\alpha n_a$  were obtained at a DME. As seen from Figure 3, a drawn out polarographic wave is obtained whose shape is that of an irreversible charge transfer<sup>13</sup> ( $E_{3/4} - E_{1/4} = 120$  mV). Characteristic plots of  $E$  vs.  $\log i/(i_d - i)$  gave a slope of 155 mV from which a similar  $\alpha n_a$  of 0.38 was calculated.

**Controlled Potential Electrolysis.** In order to verify the overall number of electrons in each step,  $\text{Rh}_2(\text{O}_2\text{CR})_4$  was reduced and oxidized at controlled potential and the cyclic voltammograms were recorded after total electrolysis. Controlled potential oxidation at potentials 200 mV more anodic than  $E_{1/2}$  showed that an overall 1.0 electron/dimeric unit was abstracted as the solution changed from green to brown. This reaction was totally reversible as evidenced by the fact that rereduction could be accomplished at +0.6 V with the addition of 1.0 electron/dimer, to produce the original green solution. Cyclic voltammetry of the oxidized species gave identical current-voltage curves as those obtained from the original unoxidized neutral complex.

Controlled potential reduction at potentials 150 mV more cathodic than  $E_{1/2}$  in  $\text{Me}_2\text{SO}$  appeared to involve several slow steps. Electronic integration of the current-time curve showed the addition of 2.5 electrons to the neutral  $\text{Rh}_2(\text{O}_2\text{CR})_4$ . Upon termination of the electrolysis, no reverse oxidation could be obtained, in agreement with the results obtained by cyclic voltammetry.

**Substituent and Solvent Effects of Redox Reactions.** As the R group was varied in Figure 1, little change was observed in peak geometry of either the oxidation or the reduction process. There did exist, however, a shift in both the oxidation and the reduction potentials such that electron-donating groups produced easier oxidations and more difficult reductions and electron-withdrawing groups had the opposite effect. The

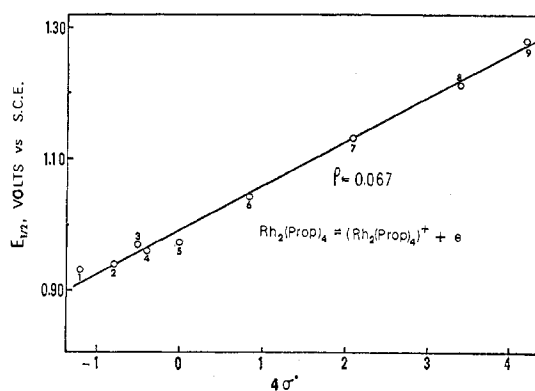


**Figure 4.** Linear free energy plot of  $E_{1/2}$  vs.  $4\sigma^*$  for electrooxidation of  $\text{Rh}_2(\text{O}_2\text{CR})_4$  in DMF. Numbers correspond to substituents given in Table I.

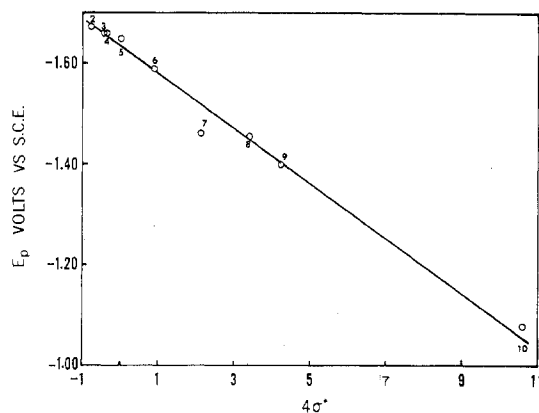


**Figure 5.** Linear free energy plot of  $E_{1/2}$  vs.  $4\sigma^*$  for electroreduction of  $\text{Rh}_2(\text{O}_2\text{CR})_4$  in  $\text{Me}_2\text{SO}$ . Numbers correspond to substituents given in Table I.

magnitude of the interaction can be quantitated by the linear free energy relationship<sup>15</sup>

$$\Delta E_{1/2} = 4\sigma^* \rho \quad (2)$$

where  $4\sigma^*$  is the total substituent constant representing the sum of the inductive or polar effects<sup>14</sup> of all substituents and  $\rho$ , the reaction constant, given in volts, measures the sensitivity of the electron-transfer reaction to the polar effect of the substituents. In this equation  $4\sigma^*$  is utilized since there are four substituted groups.

Figure 4 illustrates a plot of the reversible half-wave potentials for oxidation of various  $\text{Rh}_2(\text{O}_2\text{CR})_4$  complexes in DMF vs.  $4\sigma^*$ , while Figure 5 illustrates a similar plot of  $E_p$  for the reduction of  $\text{Rh}_2(\text{O}_2\text{CR})_4$  in  $\text{Me}_2\text{SO}$ . In both cases linear plots are obtained. The reaction constant,  $\rho$ , is the slope of the line constructed by a least-squares best fit program. Linearity of  $E_{1/2}$  or  $E_p$  vs.  $4\sigma^*$  in both cases indicates that an identical oxidation or reduction mechanism is operative throughout the series of compounds.<sup>15</sup>

The solvent was then changed in order to investigate the effect of polarity and axial ligand complexation on the electrode reactions. These solvents varied from the nonbonding  $\text{CH}_2\text{Cl}_2$  to the strongly bonding pyridine and  $\text{Me}_2\text{SO}$ . On changing from one nonaqueous solvent to another, shifts of potentials were observed similar to those obtained on changing the R group. The most positive oxidation potential was measured in  $\text{CH}_2\text{Cl}_2$  while the most negative was in pyridine. This ease of oxidation is a function of both the solvent properties and its ability to stabilize the oxidized product by bonding at the axial positions. This relationship is shown in Figure 6 where the half-wave potentials of  $\text{Rh}_2(\text{O}_2\text{CCH}_2\text{CH}_3)_4$  are plotted vs. the donor number of the solvent to yield an

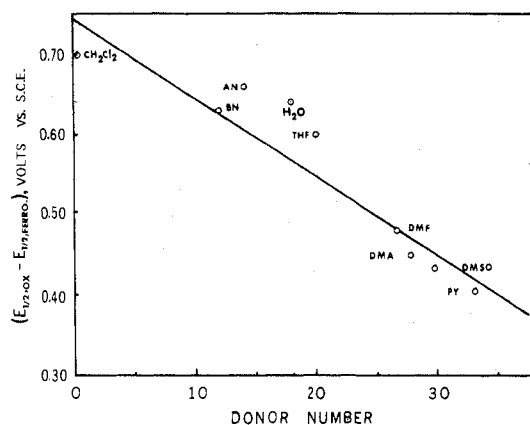


Figure 6. Plot of reversible half-wave potential for oxidation of  $\text{Rh}_2(\text{O}_2\text{CC}_2\text{H}_5)_4$  vs. Gutmann donor numbers. Values of  $E_{1/2}$  are vs. the half-wave potentials of ferrocene in the same solvent (AN = acetonitrile, BN = benzonitrile).

Table II. Reaction Constants in Different Solvents<sup>a</sup>

Solvent	$\rho$ , V, for oxidation	$\rho$ , V, for reduction
$\text{CH}_2\text{Cl}_2$	0.064	
DMF	0.067	
$\text{CH}_3\text{CN}$	0.084	
$\text{Me}_2\text{SO}$		0.060

<sup>a</sup> Standard deviation =  $\pm 0.004$ .

Table III. Potentials for Oxidation and Reduction in  $\text{H}_2\text{O}$ -0.1 M KCl

Complex	$E_{1/2}$ , V, for reduction	$E_{1/2}$ , V, for oxidation
$\text{Rh}_2(\text{O}_2\text{CCH}_2\text{OCH}_3)_4$	-0.79	
$\text{Rh}_2(\text{O}_2\text{CCH}_3)_4$	-1.08	+1.02
$\text{Rh}_2(\text{O}_2\text{CCH}_2\text{CH}_3)_4$	-1.06	+0.99
$\text{Rh}_2(\text{O}_2\text{CCH}_2\text{CH}_2\text{CH}_3)_4$	-1.06	+1.00

almost linear relationship. In this figure, the actual potentials have been plotted vs. the half-wave potentials of ferrocene/ferrocinium redox couple in order to eliminate contributions due to liquid junction potentials.<sup>13</sup>

Linear free energy plots were obtained in all solvents and reaction constants,  $\rho$ , tabulated in Table II. No significant changes were observed in the electrooxidation mechanisms as a function of changing solvents. This was not the case, however, for the electroreductions, where potentials obtained in aqueous solutions differed significantly from those in nonaqueous media. Similar to reactions in nonaqueous media, an irreversible reduction was obtained, but the potential was, in this case, some 400 mV more anodic than that predicted from the simple plot of  $E_p$  vs. donor number. No deviations were observed for the oxidation peaks so that the net effect of going from a nonaqueous solvent to water was to decrease the distance between the HOMO and the LUMO by 0.4 V from the  $2.0 \pm 0.1$  V obtained for all other solvents. The potentials for oxidation and reduction are given in Table III for the four compounds which were soluble in aqueous solution. In this table half-wave potentials are listed for oxidations and reductions of  $\text{Rh}_2(\text{O}_2\text{CR})_4$  where R corresponds to the substituents  $\text{CH}_3$ ,  $\text{C}_2\text{H}_5$ ,  $\text{C}_3\text{H}_7$ , and  $\text{CH}_3\text{OCH}_2$ .

For reversible electrode reactions where the diffusion coefficients of the oxidized and reduced forms are equal, the polarographic half-wave potential  $E_{1/2}$  may be exchanged with the thermodynamically significant  $E^\circ$ . This is not true for irreversible electrode reactions where the polarographic potential has no thermodynamic significance and is displaced from the standard potential as a function of  $\alpha n$ , the drop time,

$t$ , and the electron-transfer rate constants,  $k^\circ$ .<sup>13</sup>

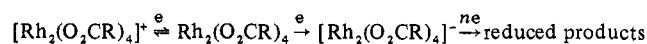
$$E_{1/2} = E^\circ + \frac{0.059}{\alpha n_a} \log \frac{1.349 k^\circ t^{1/2}}{D_0^{1/2}} \quad (3)$$

In the above equation  $D_0$  is the diffusion coefficient of the oxidized species. Since  $k^\circ$  is not known, we cannot estimate  $E^\circ$  and only know that it is more positive than  $E_{1/2}$ .

Cyclic voltammograms of the reduction could not be obtained at a platinum electrode in  $\text{H}_2\text{O}$  due to the evolution of  $\text{H}_2$  at a potential more positive than rhodium reduction. Thus, all values of  $E_{1/2}$  are those obtained at the DME and correspond to that point where the current is half the diffusion current, i.e., at the inflection point of the wave. Although no thermodynamic significance may be placed on the absolute value of  $E_{1/2}$ , predictions based on changes of half-wave potential with structure should still be valid, if  $\alpha n$  is invariant for each compound in the series. This was the case observed.

### Discussion

Based on the data the following mechanism is proposed for oxidation-reduction of  $\text{Rh}_2(\text{O}_2\text{CR})_4$ :



The electrochemical oxidation of tetra- $\mu$ -carboxylato-dirhodium(II) involves a one-electron abstraction to yield a singly positive dimeric complex. The  $E_{1/2} = 1.02$  V for the oxidation of  $\text{Rh}_2(\text{O}_2\text{CCH}_3)_4$  in  $\text{H}_2\text{O}$ , 0.1 M KCl (Table III), is within 20 mV of the value reported by Taube and co-workers<sup>6</sup> (1.225 V vs. NHE or 1.000 V vs. SCE) in 0.1 M  $\text{H}_2\text{SO}_4$  and indicates a lack of pH dependence on the oxidation. Visible and UV spectral properties of the complex are similar to those reported previously for  $\text{Rh}_2(\text{O}_2\text{CCH}_3)_4$  and  $[\text{Rh}_2(\text{O}_2\text{CCH}_3)_4]^+$ .<sup>5,6</sup>

There was no indication that the dimer cleaved upon electrooxidation and the lack of pH dependence lends support to the fact that the cage structure was not destroyed. The oxidized product appeared stable (as judged by the absorption spectra) for several hours but after this time appeared to spontaneously revert to the original neutral complex. The oxidized product,  $[\text{Rh}_2(\text{O}_2\text{CR})_4]^+$ , is electrochemically stable up to +1.7 V in  $\text{CH}_2\text{Cl}_2$  (slightly less in other solvents) and a further oxidation to yield rhodium(III) dimers was not obtained up to the potential limit of the solvent.

Under all conditions, the initial step in the electroreduction was the rate-controlling addition of a single electron. The evidence that electroreduction involves initially a single electron transfer to yield  $[\text{Rh}_2(\text{O}_2\text{CR})_4]^-$  comes directly from the shape of the current-voltage curves. All of the complexes in Table I gave irreversible electrode reactions in the solvents of Table III. Values of  $\alpha n_a = 0.38 \pm 0.05$  were invariably calculated from which an  $\alpha = 0.38 \pm 0.05$  and an  $n_a = 1$  is obtained. (The alternate explanation of  $\alpha = 0.19$  and  $n_a = 2$  seems unlikely in view of the fact that  $\alpha$  is usually between 0.3 and 0.7 and most often is about 0.5.<sup>13</sup>)

The singly reduced complex,  $[(\text{Rh}_2\text{O}_2\text{CR})_4]^-$ , is not stable but is immediately reduced by one or more electrons to yield the final complex. From the polarographic data, a diffusion current constant,  $I_d = 2.70$ , was calculated from which a value of  $nD^{1/2} = 4.28 \times 10^{-3}$  could be extracted where  $D$  is the diffusion coefficient in  $\text{cm}^2/\text{s}$  and  $n$  the overall number of electrons in the reaction. Assuming a diffusion coefficient in the range of  $1.6 \times 10^{-6}$  to  $4.9 \times 10^{-6}$   $\text{cm}^2/\text{s}$ , one can calculate that  $n$  is in the range of 2-3. This is exactly the range obtained from the coulometry.

No new reverse oxidations were obtained after total controlled reduction. This indicates the formation of an extremely stable monomeric Rh(I) complex or reduced dimer species. We did not observe the formation of a Rh(0) complex in  $\text{Me}_2\text{SO}$  solution. The final reduced yellow product had no

distinct features in the visible spectrum and possessed a high charge-transfer band characteristic of Rh(I).

**Solvent Effects.** In Figure 6, we have shown the effect of different solvents on the oxidation of  $\text{Rh}_2(\text{O}_2\text{CCH}_2\text{CH}_3)_4$ . The donor number, or the solvent donicity,<sup>16</sup> can be taken as a measure of the interaction of the axial ligands with the  $\text{Rh}^{\text{II}}$  ions in  $\text{Rh}_2(\text{O}_2\text{CR})_4$ , provided the starting complex is without any axial ligands.<sup>16,17</sup> This criterion is met in our study. All of the rhodium(II) carboxylates were desolvated by drying in a vacuum oven at about 80 °C for 2 h.

Returning to Figure 6, we see that the oxidation process becomes more favorable as the interaction of the axial group becomes stronger. This shift of potential with solvent donicity is an indication that the HOMO levels are destabilized with increasing ligand binding ability. Since  $\text{Rh}_2(\text{O}_2\text{CCH}_2\text{CH}_3)_4$  is a soft acid, it forms stronger axial bonds with ligands having  $\pi$ -acceptor ability. The  $\sigma$  interaction with pyridine, for example, is largely augmented by its synergistic  $\pi$ -acceptor ability. This will probably destabilize both the unoccupied  $\sigma^*$  levels and also the  $\pi^*$  levels,<sup>19</sup> but the symmetry consideration predicts the latter will be affected to a smaller extent than the former. This is confirmed by the fact that no linear relationship existed between the half-wave potentials and the wavelengths or molar absorptivity of spectral transitions in different solvents.

We like to report in this connection the thermodynamic stabilities of the adducts of  $\text{Rh}_2(\text{O}_2\text{CCH}_2\text{CH}_3)_4$  with pyridine and  $\text{Me}_2\text{SO}$  on one hand and with acetonitrile and carbon monoxide on the other. Whereas the former two maintain their stability in the solid state and even at quite high temperature, the existence of the latter two is detected only in solution.<sup>20</sup> Thus the purple solution of  $\text{Rh}_2(\text{O}_2\text{CCH}_2\text{CH}_3)_4$  in  $\text{CH}_3\text{CN}$ , which obviously contains the Rh(II) carboxylate in the form of its diadduct, reverts to the green starting material on evaporation of the solvent. The same is also true for carbonyl diadduct, which is formed when CO is passed through a solution of  $\text{Rh}_2(\text{O}_2\text{CR})_4$  in  $\text{CH}_2\text{Cl}_2$ . All these observations indicate that the Rh-axial ligand bond is comprised of essentially a  $\sigma$  interaction, which, however, is enhanced by the  $\pi$ -acceptor ability of the ligand.

**Substituent Effect.** One of the objectives of this study was to monitor the change in redox potentials and mechanisms of the electron-transfer reactions of  $\text{Rh}_2(\text{O}_2\text{CR})_4$  with the variation of the R group. The results of our investigations on various carboxylates in different solvents are shown in Figures 4 and 5. Only the polar substituent constants of Taft<sup>14</sup> were found to bear a linear relationship with the half-wave potentials. This linear relationship indicates that electron-donating substituents (with low or negative  $\sigma^*$  values) help to stabilize the higher oxidation state of the metal. The potential shift for the reduction of these compounds (Figure 5) may be taken as a general measure of their relative acidity toward adduct formation. With a strong electron-withdrawing group like  $\text{CF}_3$ , the lower oxidation state is stabilized to such an extent that no oxidation step can be observed for  $\text{Rh}_2(\text{O}_2\text{C}-\text{CF}_3)_4$  up to the positive end of the potential limit of the solvents. On the other hand the reduction of this complex is favored by about 500 mV compared to  $\text{Rh}_2(\text{O}_2\text{CCH}_3)_4$ . The spectral properties of the  $\text{Me}_2\text{SO}$  adducts also show that, with the exception of  $\text{Rh}_2(\text{O}_2\text{CCF}_3)_4$ , all other rhodium(II) carboxylates studied are soft acids in that they bind with  $\text{S}^-$

$\text{Me}_2\text{SO}$ , whereas  $\text{Rh}_2(\text{O}_2\text{CCF}_3)_4$  binds with  $\text{O}^{2-}$ .

These observations suggest that electronegative groups stabilize both the HOMO and LUMO of the Rh-Rh bonding scheme. The photoelectron spectra of some  $\text{Mo}_2(\text{O}_2\text{CR})_4$  (for which  $\sigma_{\text{d}_{xy}}$  is HOMO and  $\delta^*_{\text{d}_{xy}}$  is LUMO) show that both the  $\delta_{\text{d}_{xy}}$  and  $\pi_{\text{d}_{xz},\text{d}_{yz}}$  levels are stabilized by increasing electron-withdrawing ability of R group.<sup>18</sup> But how the antibonding orbitals are also equally affected in the same direction is hard to visualize. Apparently all of the MO levels are more or less equally stabilized by a change to more electronegative substituent. Thus, from an inspection of Table II, and comparison of Figures 4 and 5, we see that the difference between the oxidation and reduction potentials remains essentially constant from compound to compound.

The reaction constants,  $\rho$  values, in different solvents are given in Table II. For the electron-transfer reactions in  $\text{CH}_2\text{Cl}_2$ , DMF, and  $\text{Me}_2\text{SO}$ , these are reasonably constant at  $0.064 \pm 0.004$  V. In these solvents, therefore, the reaction follows a similar mechanism. It is interesting to note that in  $\text{Me}_2\text{SO}$ , even where there is a change of donor atoms from sulfur to oxygen, the reaction proceeds according to the same mechanism. In  $\text{CH}_3\text{CN}$ ,  $\rho = 0.084 \pm 0.004$  V. This slightly higher value in acetonitrile when compared to  $\text{Me}_2\text{SO}$  may indicate that the reaction in acetonitrile is more sensitive to the nature of the substituents than in any other solvent. This is probably an indication that the axial bonding of  $\text{Rh}_2(\text{O}_2\text{CR})_4$  with  $\text{CH}_3\text{CN}$  involves some  $\pi$  interaction which is significantly influenced by the nature of the R group in the bridging acid.

**Acknowledgment.** This work was supported by Grant CA-13817 from the National Cancer Institute, National Institutes of Health.

**Registry No.** 1, 65545-21-3; 2, 65545-22-4; 3, 56281-34-6; 4, 31126-81-5; 5, 15956-28-2; 6, 65516-94-1; 7, 59188-11-3; 8, 65516-95-2; 9, 65516-96-3; 10, 31126-95-1.

## References and Notes

- (1) R. G. Hughes, J. L. Bear, and A. P. Kimball, *Proc. Am. Assoc. Cancer Res.*, **13**, 120 (1972).
- (2) A. Erck, L. Rainen, J. Whitleyman, I. Chang, A. P. Kimball, and J. L. Bear, *Proc. Soc. Exp. Biol. Med.*, **145**, 1278 (1974).
- (3) J. L. Bear, H. B. Gray, Jr., L. Rainen, I. M. Chang, R. Howard, G. Serio, and A. P. Kimball, *Cancer Chemother. Rep.*, **59**, 611 (1975).
- (4) R. A. Howard, T. G. Spring, and J. L. Bear, *Cancer Res.*, **36**, 4402 (1976).
- (5) C. R. Wilson and H. Taube, *Inorg. Chem.*, **14**, 2276 (1975).
- (6) C. R. Wilson and H. Taube, *Inorg. Chem.*, **14**, 205 (1975).
- (7) R. D. Cannon, D. B. Powell, K. Sarawek, and J. S. Stillman, *J. Chem. Soc., Chem. Commun.*, 31 (1976).
- (8) M. Moszner and J. J. Ziolkowski, *Bull. Acad. Pol. Sci., Ser. Sci. Chim.*, **24**, 433 (1976).
- (9) J. Kitchens and J. L. Bear, *J. Inorg. Nucl. Chem.*, **31**, 2415 (1969).
- (10) K. Das, E. L. Simmons, and J. L. Bear, *Inorg. Chem.*, **16**, 1268 (1977).
- (11) R. N. Adams, "Electrochemistry at Solid Electrodes", Marcel Dekker, New York, N.Y., 1969.
- (12) R. S. Nicholson and I. Shain, *Anal. Chem.*, **36**, 706 (1964).
- (13) L. Meites, "Polarographic Techniques", 2nd ed, Interscience, New York, N.Y., 1965.
- (14) R. W. Taft, Jr., in "Steric Effects in Organic Chemistry", M. S. Newman, Ed., Wiley, New York, N.Y., 1956.
- (15) P. Zuman, "Substituent Effects in Organic Polarography", Plenum Publishing Co., New York, N.Y., 1967.
- (16) V. Gutmann, *Electrochim. Acta*, **21**, 661 (1976).
- (17) D. Sawyer and J. L. Roberts, "Experimental Electrochemistry for Chemists", Interscience, New York, N.Y., 1974.
- (18) F. A. Cotton, J. G. Norman, Jr., B. R. Stults, and T. R. Webb, *J. Coord. Chem.*, **5**, 217 (1976).
- (19) Dr. Norman informed us through a private communication that in Rh-Rh bonding scheme  $\sigma^*$  and  $\pi^*$  are LUMO and HOMO, respectively.
- (20) K. Das and J. L. Bear, unpublished results.
- (21) J. Kitchens and J. L. Bear, *J. Inorg. Nucl. Chem.*, **32**, 49 (1970).